Available online at www.sciencedirect.com
SCIENCE DIRECT®
PERGAMON
International Journal of Heat and Mass Transfer 46 (2003) 1613–1627
International Journal of HEAT and MASS TRANSFER
www.elsevier.com/locate/ijhmt

Direct numerical simulation of heated vertical air flows in fully developed turbulent mixed convection

Jongwoo You [1], Jung Y. Yoo *, Haecheon Choi [1]

School of Mechanical and Aerospace Engineering, Seoul National University, Seoul 151-742, South Korea

Received 24 May 2000; received in revised form 11 September 2002

Abstract

Turbulent mixed convection associated with upward and downward flows in heated vertical tubes is investigated using the direct numerical simulation technique. With increasing heat flux, the skin friction first decreases and then increases in upward heated flow, while it changes little in downward heated flow. The heat transfer coefficient exhibits a similar trend in upward heated flow, but it monotonically increases in downward heated flow. The log laws of the mean-velocity and temperature profiles are valid for downward heated flow but not for upward heated flow. Finally, the influence of buoyancy on turbulent transport of momentum and heat is elucidated by the 'external' and 'structural' effects.

1. Introduction

Mixed convection in a heated or cooled vertical tube is encountered in many engineering applications, such as nuclear reactor cooling systems, heat exchangers and solar power generators, which operate in laminar, transition, or low-Reynolds-number turbulent flow regimes, where buoyancy strongly affects velocity and temperature fields [1].

Since the heat transfer characteristics of turbulent mixed convection have received more attention than the flow characteristics, the literature contains fairly accurate correlations of the heat transfer coefficient. In general, with increasing heat flux, the Nusselt number Nu first decreases and then increases sharply in upward heated flow, but it monotonically increases in downward heated flow. The review of Jackson et al. [2] gives a most comprehensive account of this subject.

There have been several studies that discussed the buoyancy effect on the skin friction in turbulent mixed convection. Petukhov and Strigin [3] measured the friction pressure drop in upward heated water flow, and found a monotonically increasing skin friction with increasing heat flux. In their studies on upward heated air flow, Carr et al. [4] and Polyakov and Shindin [5] measured the velocity profiles using a hot-wire anemometry and an LDA, respectively, and calculated the skin friction from the convective velocity gradients at specific axial positions. They found that the skin friction first decreased and then increased slightly with increasing heat flux. On the other hand, Abdelmeguid and Spalding [6] employed a finite-difference forward-marching procedure with a two-equation turbulence model to predict turbulent flow and heat transfer in vertical tubes under the influence of buoyancy. They reported that the skin friction increased monotonically in upward heated flow. Parlatan et al. [1] measured the total pressure drop in heated water flow by a differential pressure transducer, and reported that the skin friction increased monotonically with increasing heat flux in upward heated flow, with the suggestion that the disagreement among the previous studies might be due to the fact that the velocity measurements were not taken in the near-wall region ($y^+ \leqslant 30$) in the experiments of Carr et al. [4] and Polyakov and Shindin [5].

In downward heated flow, the skin friction was found to decrease slightly by Abdelmeguid and Spalding [6].

* Corresponding author. Tel.: +82-2-880-7112; fax: +82-2-888-2968.
E-mail address: jyyoo@plaza.snu.ac.kr (J.Y. Yoo).
[1] Also at National CRI Center for Turbulence and Flow Control Research, Institute of Advanced Machinery and Design, Seoul National University.

0017-9310/03/$ - see front matter © 2002 Elsevier Science Ltd. All rights reserved.
PII: S0017-9310(02)00442-8

Nomenclature

Bo	buoyancy number, $8\times10^4\cdot16Gr_q/((2\cdot Re)^{3.425}Pr^{0.8})$
C_f	skin-friction coefficient, $\tau_w/(0.5\rho U_b^2)$
C_p	specific heat at constant pressure
Gr_q	Grashof number, $g\beta q_w R^4/kv^2$
g	gravitational acceleration
h	heat transfer coefficient, $q_w/(T_w-T_b)$
k	thermal conductivity; turbulent kinetic energy
Nu	Nusselt number, $h\cdot 2R/k$
Pr	Prandtl number
p	pressure
q_w	wall heat flux
R	tube radius
r,ϕ,x	cylindrical coordinates
Re	Reynolds number, U_bR/v
T_b	bulk temperature
T_w	wall temperature
T_τ	non-dimensional temperature, $q_w/(\rho C_p u_\tau)$
t	temperature
U_b	bulk velocity
u_r,u_ϕ,u_x	non-dimensional velocity components in cylindrical coordinates
u_τ	wall-shear velocity, $(\tau_w/\rho)^{1/2}$
y	wall-normal distance from the wall

Greek symbols

β	coefficient of volume expansion
ε	dissipation
θ	non-dimensional temperature, $(T_w-t)/(T_w-T_b)$
v	kinematic viscosity
ω_x	streamwise vorticity
ρ	density
τ	non-dimensional time
τ_w	wall-shear stress
φ	non-dimensional temperature, $(T_w-t)/(q_wR/k)$

Subscripts

$()_{rms}$	root-mean-square fluctuation
$()_o$	value for forced convection

Superscripts

$\overline{()}$	average over the $x-\phi$ plane and time
$()'$	fluctuation
$()^+$	value in wall unit: $y^+=yu_\tau/v$, $u_x^+=u_x/u_\tau$ and $\theta^+=(T_w-t)/T_\tau$

Easby [7] obtained the skin friction from the manometer-measured total pressure drop in the heated downward flow of pressurized nitrogen and showed that it decreased by as much as 20% with increasing heat flux. Parlatan et al. [1] obtained 25% decrease in the skin friction in downward heated water flow.

Kasagi and Nishimura [8] investigated the turbulent mixed convection in a fully developed upward flow between two vertical parallel plates kept at different temperatures. At the cold wall, the skin friction decreased with increasing heat flux, whereas the opposite is observed at the hot wall.

As mentioned above, the previous results on heated vertical flows are quite inconclusive and our understanding of the flow and heat transfer characteristics in turbulent mixed convection regime is still limited. Therefore, the objective of the present study is to investigate the buoyancy effect on turbulent transport of momentum and heat in heated vertical tubes using direct numerical simulation.

2. Numerical details

We consider upward and downward flows in vertical tubes heated with uniform wall heat flux, q_w. The streamwise (x) direction is opposite to that of the gravitational acceleration for upward heated flow and coincident with it for downward heated flow.

The governing equations are the continuity, incompressible Navier–Stokes and energy equations:

$$\frac{\partial u_x}{\partial x}+\frac{1}{r}\frac{\partial(ru_r)}{\partial r}+\frac{1}{r}\frac{\partial u_\phi}{\partial\phi}=0, \tag{1}$$

$$\frac{\partial u_x}{\partial\tau}+u_x\frac{\partial u_x}{\partial x}+u_r\frac{\partial u_x}{\partial r}+\frac{u_\phi}{r}\frac{\partial u_x}{\partial\phi}=\frac{1}{Re}\left[\frac{\partial^2u_x}{\partial x^2}+\frac{\partial}{\partial r}\left(\frac{1}{r}\frac{\partial(ru_x)}{\partial r}\right)+\frac{1}{r^2}\frac{\partial^2u_x}{\partial\phi^2}\right]-\frac{\partial p}{\partial x}\mp\frac{Gr_q}{Re^2}\varphi, \tag{2}$$

$$\frac{\partial u_r}{\partial\tau}+u_x\frac{\partial u_r}{\partial x}+u_r\frac{\partial u_r}{\partial r}+\frac{u_\phi}{r}\frac{\partial u_r}{\partial\phi}-\frac{u_\phi^2}{r}=-\frac{\partial p}{\partial r}+\frac{1}{Re}\left[\frac{\partial^2u_r}{\partial x^2}+\frac{\partial}{\partial r}\left(\frac{1}{r}\frac{\partial(ru_r)}{\partial r}\right)+\frac{1}{r^2}\frac{\partial^2u_r}{\partial\phi^2}-\frac{2}{r^2}\frac{\partial u_\phi}{\partial\phi}\right], \tag{3}$$

$$\frac{\partial u_\phi}{\partial \tau} + u_x \frac{\partial u_\phi}{\partial x} + u_r \frac{\partial u_\phi}{\partial r} + \frac{u_\phi}{r}\frac{\partial u_\phi}{\partial \phi} + \frac{u_r u_\phi}{r} = -\frac{1}{r}\frac{\partial p}{\partial \phi} + \frac{1}{Re}\left[\frac{\partial^2 u_\phi}{\partial x^2} + \frac{\partial}{\partial r}\left(\frac{1}{r}\frac{\partial (r u_\phi)}{\partial r}\right) + \frac{1}{r^2}\frac{\partial^2 u_\phi}{\partial \phi^2} + \frac{2}{r^2}\frac{\partial u_r}{\partial \phi}\right], \tag{4}$$

$$\frac{\partial \varphi}{\partial \tau} + u_x \frac{\partial \varphi}{\partial x} + u_r \frac{\partial \varphi}{\partial r} + \frac{u_\phi}{r}\frac{\partial \varphi}{\partial \phi} = \frac{1}{RePr}\left[\frac{\partial^2 \varphi}{\partial x^2} + \frac{\partial}{\partial r}\left(\frac{1}{r}\frac{\partial (r\varphi)}{\partial r}\right) + \frac{1}{r^2}\frac{\partial^2 \varphi}{\partial \phi^2}\right] + \frac{2}{RePr} u_x. \tag{5}$$

Throughout this paper the upper sign for the buoyancy term refers to upward heated flow and the lower one to downward heated flow. Note that the buoyancy term $\left(Gr_q/Re^2\varphi\right)$ appears only in the streamwise momentum equation (2). Eq. (5) is derived by introducing the definition of the dimensionless temperature φ into the energy equation and the last term appears by considering the relation between the bulk temperature and heat flux. The governing equations (1)–(5) are non-dimensionalized by U_b and R. The physical properties are regarded as constant except for the buoyancy term. In this study, air is chosen as the working fluid, so that $Pr = 0.71$.

The governing equations (1)–(5) are discretized spatially using a second-order finite volume formulation and integrated temporally by a fractional step method. Using the finite volume technique with the staggered grid system, a singularity along the centerline can be circumvented rather easily without much special effort; centerline conditions are actually not needed for any of the variables, except for u_r which can be obtained by averaging neighboring values across the centerline [9]. Also, the temporal domain decomposition method by Akselvoll and Moin [9] is used. This procedure simplifies the solution algorithm because only one component of the discretized momentum equation is non-linear in each domain. A modified third-order Runge–Kutta scheme [10] is used for the terms treated explicitly and the Crank–Nicolson method is used for the terms treated implicitly.

In this study, a constant mass flow rate is imposed throughout the computation. Thus, $Re(= U_b R/\nu)$ is fixed at 2650, which corresponds to $u_{\tau_0} R/\nu \approx 180$ in the case of forced convection. The value of Gr_q/Re^2 is taken to be less than 0.434 not to violate the Boussinesq approximation [11].

For downward heated flow, the streamwise length of the computational domain is taken to be $10R$, which corresponds to about 1800 wall units. On the other hand, much longer streamwise domain size of $30R$ is taken for upward heated flow due to the attenuation of turbulence in this flow. This streamwise length of the computational domain is sufficient to allow the two-point correlations of the root-mean-square (rms) velocity fluctuations to be nearly zero at large separation distances. The number of grid points in the x, r, and ϕ directions, respectively, is $256 \times 68 \times 128$ for downward heated flow and $512 \times 68 \times 128$ for upward heated flow. The grid spacings in wall units are $\Delta x^+ \approx 7 \sim 10.5$, $0.17 \leqslant \Delta r^+ \leqslant 5.1$, and $(\Delta\phi)^+ \approx 8.85$, based on u_{τ_0} in the case of forced convection.

3. Laminar mixed convection

In this section, we simulate laminar mixed convection for a later comparison with turbulent mixed convection, because the buoyancy effect on laminar transport of momentum and heat may be interpreted as an 'external' effect of buoyancy on turbulent transport (see Section 4.7 for more details).

Fig. 1 shows the streamwise velocity and temperature profiles in upward and downward heated flows. Analytical solutions for laminar mixed convection were reported by Hanratty et al. [12]. There is an excellent agreement between the numerical and analytical solutions.

In upward heated flow, with increasing heat flux, the peak-velocity location shifts from the tube center toward the wall and the velocity gradient near the wall becomes steeper, resulting in the increase in the skin friction (see Fig. 3a). Also, the velocity profile develops a dip at the tube center and thus shows an M-shape. The temperature gradient at the wall also increases with increasing heat flux. The mechanism for these changes can be explained as follows: with increasing heat flux the density near the wall becomes smaller so that the velocity near the wall increases while the velocity in the core region decreases because of the fixed mass flow rate. As the velocity near the wall continues to increase, the non-dimensionalized temperature gradient near the wall also increases, resulting in the increase in the Nusselt number (as will be shown later in Fig. 6a).

In downward heated flow, the velocity decreases near the wall and increases in the core region with increasing heat flux. Near the wall the velocity is retarded by the decreased density due to wall heating, and thus the skin friction decreases (see Fig. 3b). The non-dimensionalized temperature gradient also decreases with increasing heat flux, and the Nusselt number monotonically decreases (as will be shown later in Fig. 6b).

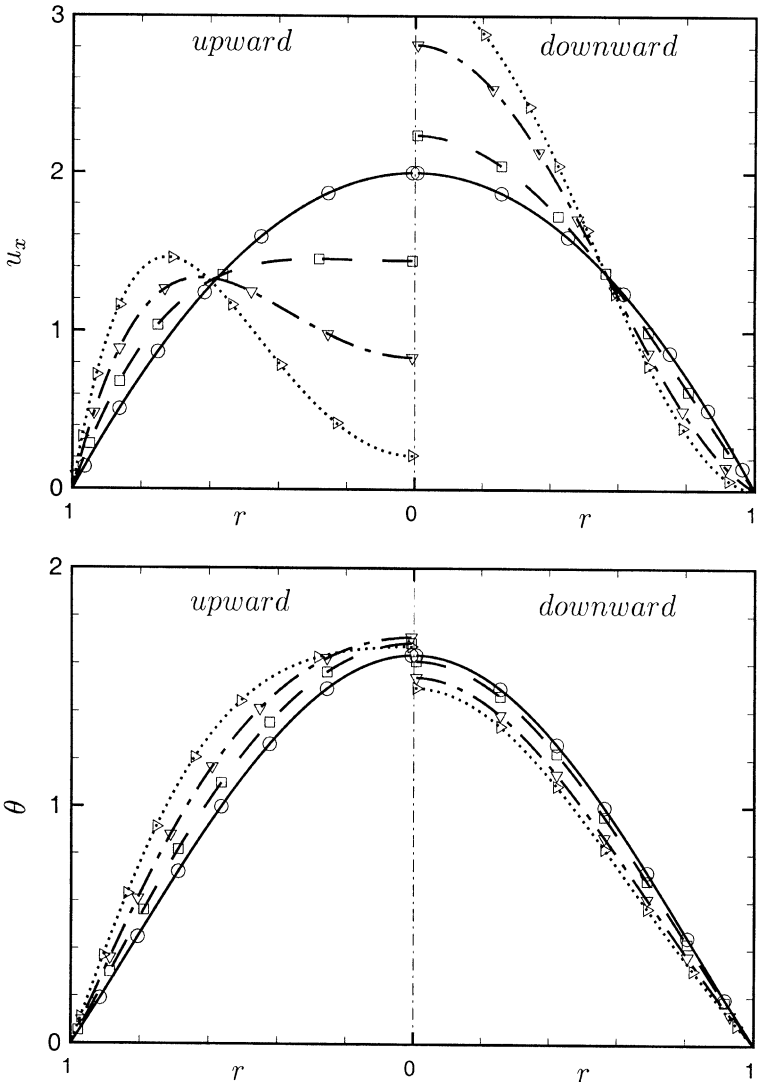

Fig. 1. Velocity and temperature profiles in laminar flow. Upward heated flow: (——) $Gr_q/Re^2 = 0$; (- - - -) 0.015; (-·-·-·-) 0.039; (· · · · · ·) 0.087. Downward heated flow: (- - - -) $Gr_q/Re^2 = 0.005$; (-·-·-·-) 0.015; (· · · · · ·) 0.019. Symbols denote analytical solutions [12].

4. Turbulent mixed convection

4.1. Mean velocity and skin friction

Fig. 2(a) shows the mean-velocity profiles plotted in global coordinates, together with previous results for forced convection [13] and mixed convection [4]. With increasing heat flux, the change in the mean-velocity profile shows a similar trend to that of Carr et al. [4]. Unlike laminar mixed convection the velocity profile near the wall does not change monotonically with increasing heat flux, i.e. the velocity near the wall first decreases and then increases. At high heat fluxes the velocity profiles show M-shapes. Similar experimental results were also obtained by Carr et al. [4] and Polyakov and Shindin [5]. In Fig. 2(b), the mean-velocity profiles are plotted in wall coordinates. It is clear that the log law is not valid any more for mixed convection in upward heated flow.

Unlike in upward heated flow, the velocity profile in downward heated flow changes monotonically with increasing heat flux. In global coordinates (Fig. 2a), the velocity near the wall changes little from that of forced convection, but the velocity decreases for $0.55 < r < 0.9$ and increases in the core region with increasing heat flux. A similar experimental result was obtained by Axcell and Hall [14] who measured velocity profiles in downward heated air flow in a vertical tube

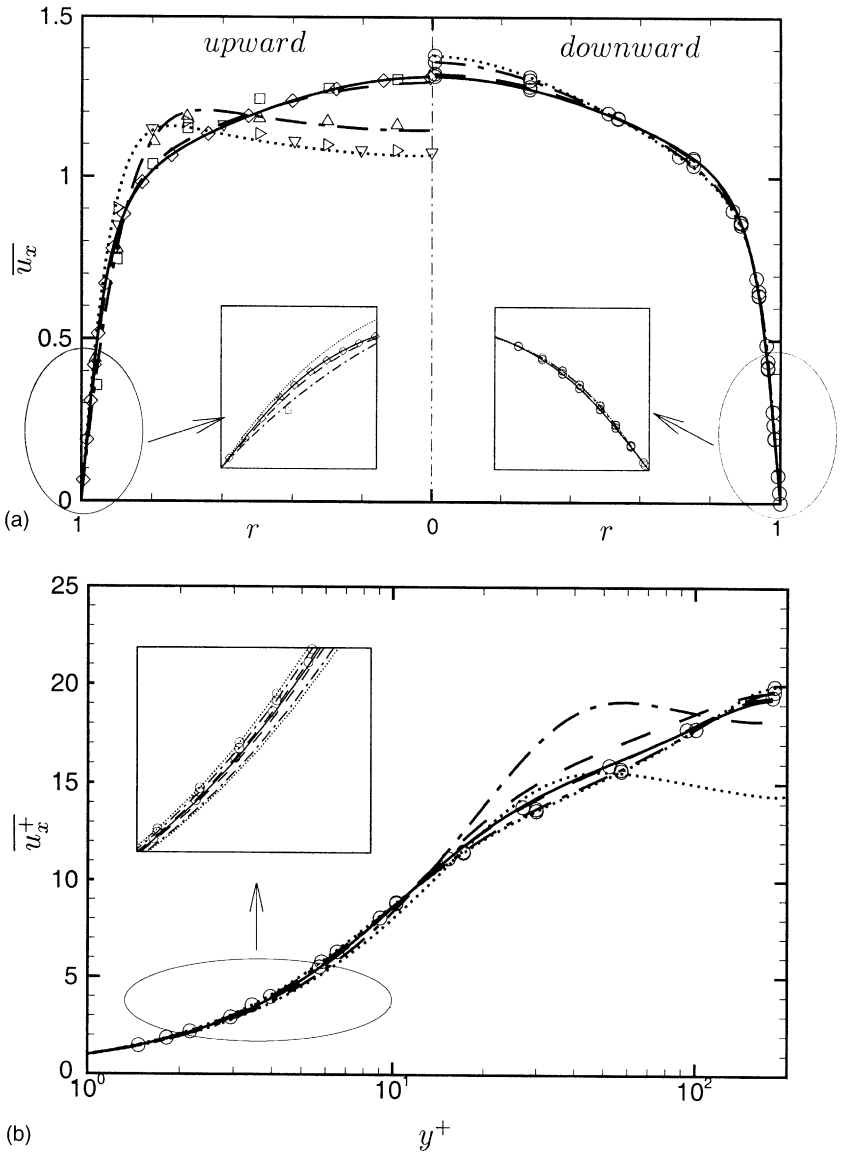

Fig. 2. Mean-velocity profiles plotted in: (a) global coordinates; (b) wall coordinates. Upward heated flow (lines without ○): (——) $Gr_q/Re^2 = 0$; (- - - -) 0.063; (-·-·-·-) 0.087; (· · · · · ·) 0.241. Symbols denote the results of Eggels et al. [13] for forced convection and Carr et al. [4] for mixed convection: (◇) $Gr_q/Re^2 = 0$; (□) 0.092; (△) 0.136; (▽) 0.184; (▷) 0.224. Downward heated flow (lines with ○): (——) $Gr_q/Re^2 = 0$; (- - - -) 0.063; (-·-·-·-) 0.241; (· · · · · ·) 0.434.

and showed that buoyancy reduced the velocity for $r > 0.65$ and increased it in the core region. However, they did not measure the velocity very near the wall, nor mention the wall shear stress. In wall coordinates (Fig. 2b), the deviation of the mean velocity from the log law is much smaller than that for upward heated flow. The velocity plotted in wall coordinates decreases for $10 < y^+ < 90$ and increases for $y^+ > 90$.

Fig. 3 shows the variation of the normalized skin friction with respect to the buoyancy number *Bo* which is widely used in the literature to represent the effect of buoyancy [15], together with other numerical and experimental results including those for the case of laminar flow. In this figure, C_{f_0} is the skin-friction coefficient for forced convection and is evaluated as 9.28×10^{-3} for turbulent flow and 3.02×10^{-3} for laminar flow. The variation of C_f/C_{f_0} with *Bo* is much larger for laminar flow than for turbulent flow. In upward heated turbulent flow the skin friction first decreases and then increases with increasing *Bo*. This behavior agrees with the experimental results of Carr et al. [4] and Polyakov and

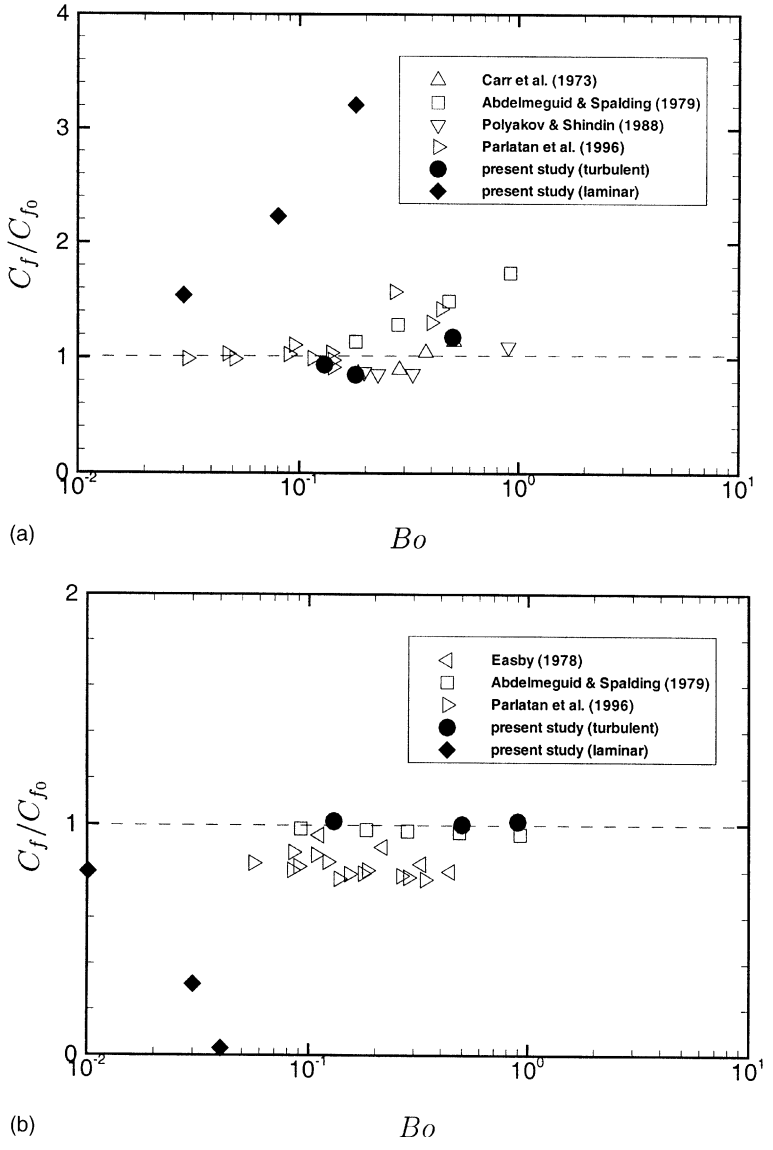

Fig. 3. Skin-friction ratio: (a) upward heated flow; (b) downward heated flow.

Shindin [5] who obtained the skin friction from the measured velocity gradient, but does not agree with the numerical result of Abdelmeguid and Spalding [6] and the experimental result of Parlatan et al. [1] who determined the skin friction from the total pressure drop measured by a differential transducer. In downward heated turbulent flow the skin friction shows little change from that for forced convection, which is in reasonable agreement with the numerical result of Abdelmeguid and Spalding [6] but not with the experimental results of Easby [7] and Parlatan et al. [1].

It is interesting to note that the variation of C_f with Bo agrees with the numerical result of Abdelmeguid and Spalding [6] for downward heated flow but not for upward heated flow. The reason for this difference is that the log law used in Abdelmeguid and Spalding [6] is more or less valid for downward heated flow, but is invalid for upward heated flow (see Fig. 2b). It should be also addressed here that the present results for C_f in both upward and downward heated flows do not agree with the experimental results obtained by using the total pressure drop, but agree with those obtained by measuring the velocity gradient in the case of upward heated flow. In experiments, it is not easy to measure the actual pressure drop corresponding to the skin-friction loss in a vertical tube due to the acceleration pressure drop between the

inlet and exit as well as the gravitational pressure drop [1,7]. Also, one needs a very long tube to obtain C_f correctly using the total pressure-drop technique.

4.2. Velocity fluctuations and Reynolds shear stress

Fig. 4 shows the rms velocity fluctuations and Reynolds shear stress plotted in global coordinates. In upward heated flow, the rms velocity fluctuations show non-monotonic behaviors: they first decrease and then recover with increasing heat flux. At $Gr_q/Re^2 = 0.087$ the reduction in the rms velocity fluctuations is significant throughout the tube, especially very near the wall. Also, the significant reduction in the peak of $u_{x_{\mathrm{rms}}}$ results in nearly constant values of $u_{x_{\mathrm{rms}}}$ across the tube cross-section, which is similar to that observed in turbulent free convection [16]. At $Gr_q/Re^2 = 0.241$ the velocity fluctuations are recovering themselves due to the increase in the shear and buoyancy productions (see Section 4.5). It is also interesting to note that two peaks exist in $u_{x_{\mathrm{rms}}}$ at high heat fluxes. In downward heated flow, the rms velocity fluctuations monotonically

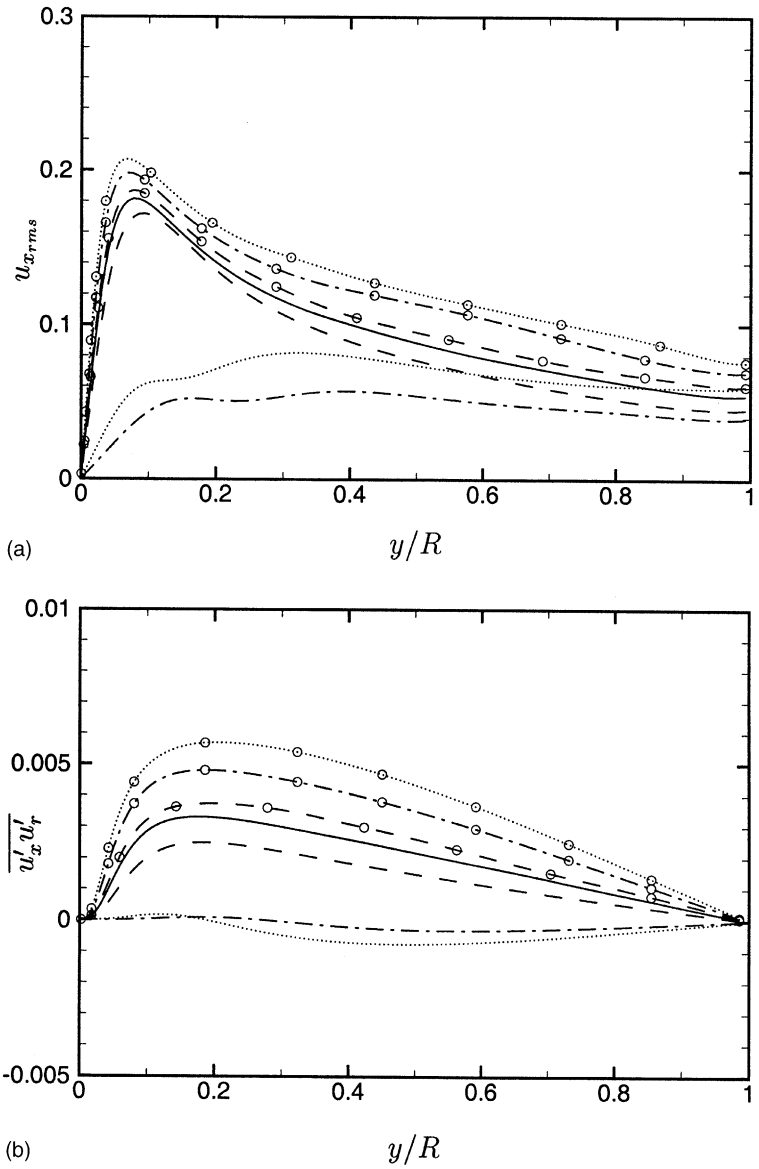

Fig. 4. (a) Root-mean-square velocity fluctuations ($u_{x_{\mathrm{rms}}}$) and (b) Reynolds shear stress ($\overline{u'_x u'_r}$) plotted in global coordinates. Upward heated flow (lines without ○): (——) $Gr_q/Re^2 = 0$; (- - - -) 0.063; (-·-·-·) 0.087; (· · · · · ·) 0.241. Downward heated flow (lines with ○): (- - - -) $Gr_q/Re^2 = 0.063$; (-·-·-·) 0.241; (· · · · · ·) 0.434.

increase with increasing heat flux. Also, the peak location moves toward the wall as Gr_q/Re^2 increases.

The Reynolds shear stress exhibits a similar trend to that of the rms velocity fluctuations. In upward heated flow, at $Gr_q/Re^2 = 0.087$ and 0.241, the Reynolds shear stress becomes negative away from the wall, which is related to the M-shape of the mean velocity profile (Fig. 2a). This negative Reynolds shear stress was also found in turbulent free convection [16].

4.3. Mean temperature and the Nusselt number

Fig. 5 shows the mean-temperature profiles in global and wall coordinates. In upward heated flow, the mean-temperature profile plotted in global coordinates does not show an M-shape, unlike the mean velocity, but its variation with increasing heat flux is non-monotonic like the variation of the mean-velocity profile. With increasing heat flux, the non-dimensional temperature

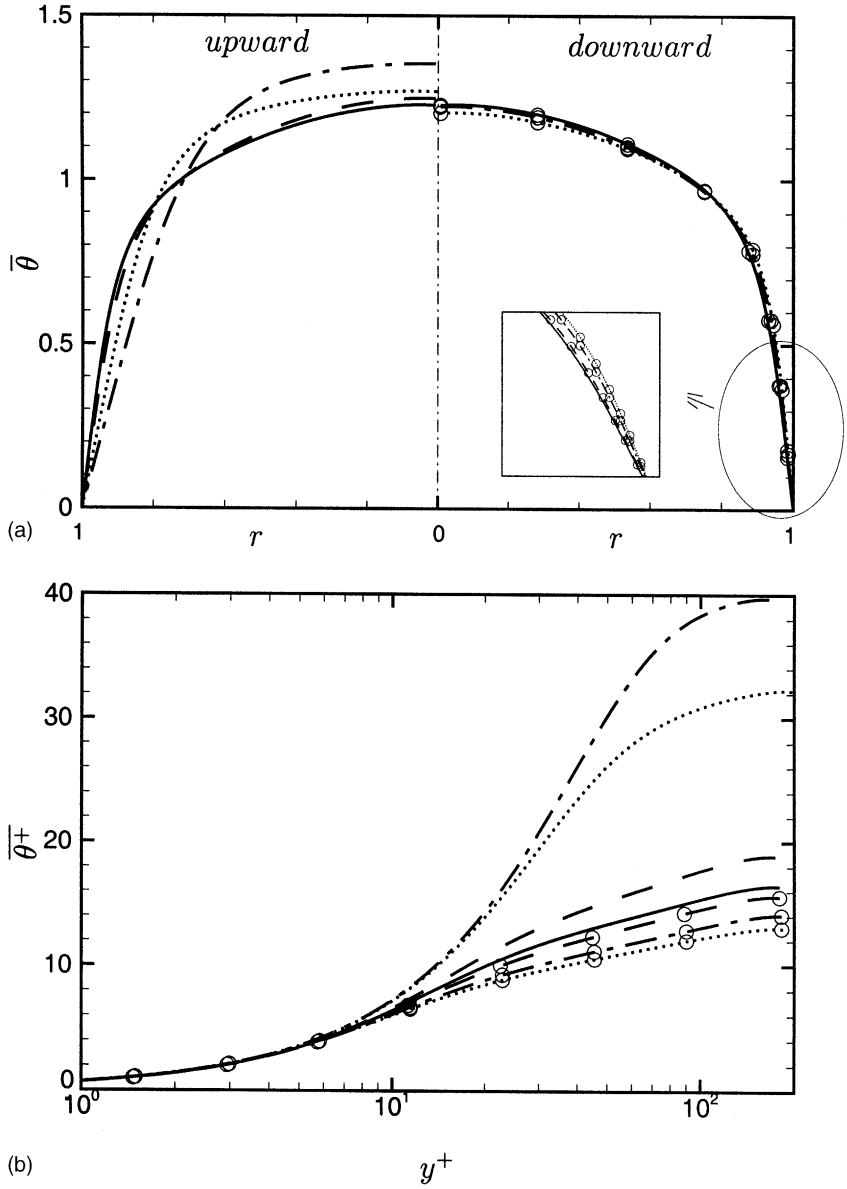

Fig. 5. Mean-temperature profiles plotted in: (a) global coordinates; (b) wall coordinates. Upward heated flow (lines without O): (——) $Gr_q/Re^2 = 0$; (- - - -) 0.063; (-·-·-·) 0.087; (· · · · · ·) 0.241. Downward heated flow (lines with O): (——) $Gr_q/Re^2 = 0$; (- - - -) 0.063; (-·-·-·) 0.241; (· · · · · ·) 0.434.

initially (i.e. at $Gr_q/Re^2 = 0.063$ and 0.087) decreases near the wall, but later (at $Gr_q/Re^2 = 0.241$) it recovers as compared with that at $Gr_q/Re^2 = 0.087$. In wall coordinates, the slope of the log law significantly changes from that for forced convection, or the log-law region nearly disappears, whereas there is little change in the viscous sublayer. In downward heated flow, the variation of the mean-temperature profile plotted in global and wall coordinates is monotonic with increasing heat flux. That is, the mean temperature increases in the near-wall region and decreases in the core region. The slope of the log law changes slightly, and the temperature shows a downward shifting in the log-law region.

Fig. 6 shows the variation of the normalized heat transfer coefficient Nu/Nu_0 with respect to the buoyancy number Bo, together with other numerical and experimental results including those for the case of laminar flow. Nu_0 is the Nusselt number for forced convection and is calculated to be 18.3 for turbulent flow and 4.36

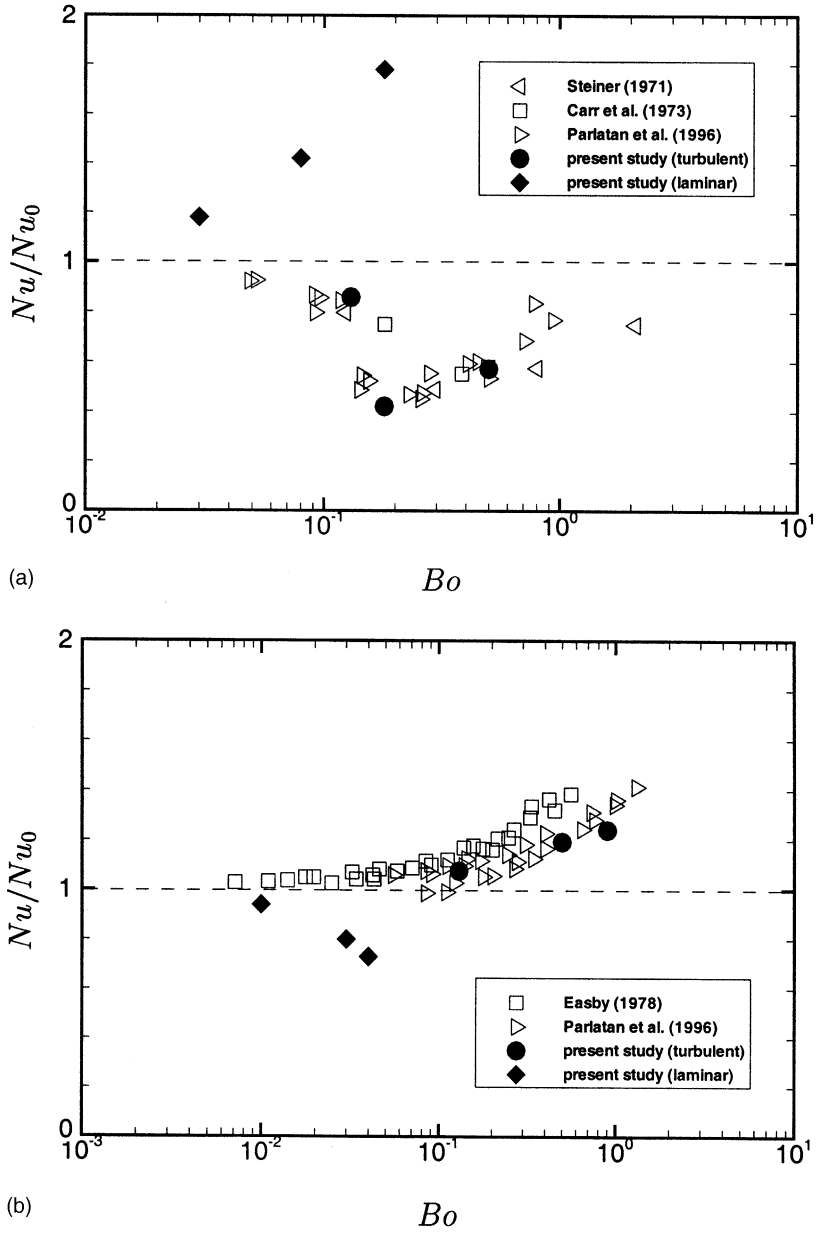

Fig. 6. Nusselt number ratio: (a) upward heated flow; (b) downward heated flow.

for laminar flow. It is interesting to note that the behavior of Nu/Nu_0 for turbulent flow is very different from that for laminar flow. That is, for the ranges of Bo investigated, Nu/Nu_0 decreases for turbulent flow but increases for laminar flow in upward heated flow, whereas the opposite is observed in downward heated flow. A more detailed discussion about this observation is made in Section 4.7. In upward heated turbulent flow, Nu rapidly decreases at $Bo \approx 0.2$, where about 50% reduction in Nu is obtained. At a higher Bo (≈ 0.5), Nu increases but still is smaller than that for forced convection. The present result is in good agreement with the existing data in the literature [1,4,17]. The behavior of Nu with increasing heat flux is in general similar to that of the skin friction shown in Fig. 3(a). However, it is notable that at $Bo \approx 0.5$, the skin friction is larger than that for forced convection, while the heat transfer rate is smaller than that for forced convection, indicating that the similarity between the velocity and temperature is not valid when the buoyancy effect becomes significant. In downward heated turbulent flow, Nu increases monotonically with increasing heat flux unlike the skin friction, again showing a dissimilarity between the velocity and temperature. The experimental data of Easby [7] and Parlatan et al. [1] also showed similar behaviors.

4.4. Temperature fluctuations and turbulent heat fluxes

Fig. 7(a) shows the rms temperature fluctuations plotted in global coordinates. In upward heated flow, the temperature fluctuations first decrease and then recover with increasing heat flux in the near-wall region. In downward heated flow, the temperature fluctuations monotonically increase with increasing heat flux in the near-wall region. By comparing Figs. 7(a) and 4(a), it is noted that the variation of θ_{rms} with increasing heat flux is not the same as that of $u_{x_{\mathrm{rms}}}$, which again shows a dissimilarity between the velocity and temperature in the presence of buoyancy.

The streamwise and wall-normal turbulent heat fluxes in upward and downward heated flows are shown in Fig. 7(b)–(c). In upward heated flow, the magnitude of the streamwise heat flux first decreases and then recovers near the wall with increasing heat flux. At $Gr_q/Re^2 = 0.087$ and 0.241, the streamwise turbulent heat flux becomes negative away from the wall, which is also related to the M-shape of the mean-velocity profile. The wall-normal turbulent heat flux also decreases and then recovers with increasing heat flux, but it is positive throughout the tube at all the heat fluxes considered. In downward heated flow, the streamwise heat flux increases in the near-wall region but changes little away from the wall. The wall-normal component also increases with increasing heat flux.

The changes in the Reynolds stresses in the presence of buoyancy may be described by the Reynolds stress equations,

$$\frac{D}{D\tau}\left(\overline{u_x'u_x'}\right) = \cdots \mp 2\frac{Gr_q}{Re^2}\overline{u_x'\varphi'}, \tag{6}$$

$$\frac{D}{D\tau}\left(\overline{u_x'u_r'}\right) = \cdots \mp \frac{Gr_q}{Re^2}\overline{u_r'\varphi'}, \tag{7}$$

where the negative and positive signs are for upward and downward heated flows, respectively, $\overline{u_x'\varphi'} = \overline{u_x'\theta'}/Nu$ and $\overline{u_r'\varphi'} = \overline{u_r'\theta'}/Nu$. Among six Reynolds stress components, only the streamwise velocity intensity and the Reynolds shear stress have direct interactions with buoyancy. It is shown in Eqs. (6) and (7) that the streamwise velocity intensity is associated with the streamwise turbulent heat flux ($\overline{u_x'\varphi'}$), and the Reynolds shear stress is related to the wall-normal turbulent heat flux ($\overline{u_r'\varphi'}$). In the case of downward heated flow, $\overline{u_x'\varphi'}$ and $\overline{u_r'\varphi'}$ are positive and thus they are considered as gains to $u_{x_{\mathrm{rms}}}$ and $\overline{u_x'u_r'}$ (see Fig. 4). On the other hand, in the case of upward heated flow, due to the negative sign in the buoyancy terms of Eq. (6), they become losses to $u_{x_{\mathrm{rms}}}$ and $\overline{u_x'u_r'}$ at low heat fluxes. However, at high heat fluxes $\overline{u_x'\varphi'}$ is negative away from the wall (Fig. 7b) and thus it acts as a gain to $u_{x_{\mathrm{rms}}}$ (see Fig. 4a), but $\overline{u_r'\varphi'}$ is still positive (Fig. 7c) and thus is again a gain to $\overline{u_x'u_r'}$ because $\overline{u_x'u_r'} < 0$ at high heat fluxes.

4.5. Turbulent kinetic energy budget

The transport equation for the turbulent kinetic energy, $k = \frac{1}{2}(\overline{u_x'^2} + \overline{u_r'^2} + \overline{u_\phi'^2})$, is expressed as:

$$\frac{Dk}{D\tau} = -\overline{u_x'u_r'}\frac{\mathrm{d}\overline{u_x}}{\mathrm{d}r} - \frac{1}{r}\frac{\mathrm{d}}{\mathrm{d}r}\left(r\overline{u_r'k}\right) - \frac{1}{r}\frac{\mathrm{d}}{\mathrm{d}r}\left(r\overline{u_r'p'}\right) + \frac{1}{Re}\left[\frac{1}{r}\frac{\mathrm{d}}{\mathrm{d}r}\left(r\frac{\mathrm{d}k}{\mathrm{d}r}\right)\right] - \epsilon \mp \frac{Gr_q}{Re^2}\overline{u_x'\varphi'}, \tag{8}$$

where ϵ is the dissipation, and the negative and positive signs are for upward and downward heated flows, respectively. Terms on the right-hand side of Eq. (8) represent the shear production, turbulent diffusion, velocity–pressure gradient, viscous diffusion, dissipation and buoyancy production. The magnitude of the buoyancy production is of special interest in this study.

Fig. 8 shows each term in Eq. (8) for upward and downward heated flows at $Gr_q/Re^2 = 0.241$. Without buoyancy ($Gr_q/Re^2 = 0$) the turbulent kinetic energy budget is largely dominated by the shear production and dissipation except in the near-wall region. Very near the wall the dissipation is balanced with the viscous diffusion and has its maximum at the wall. In upward heated flow, the dissipation has its maximum away from the wall and is nearly uniform in the core region unlike the case of forced convection. Near the wall, the buoyancy production is much smaller than the shear production and

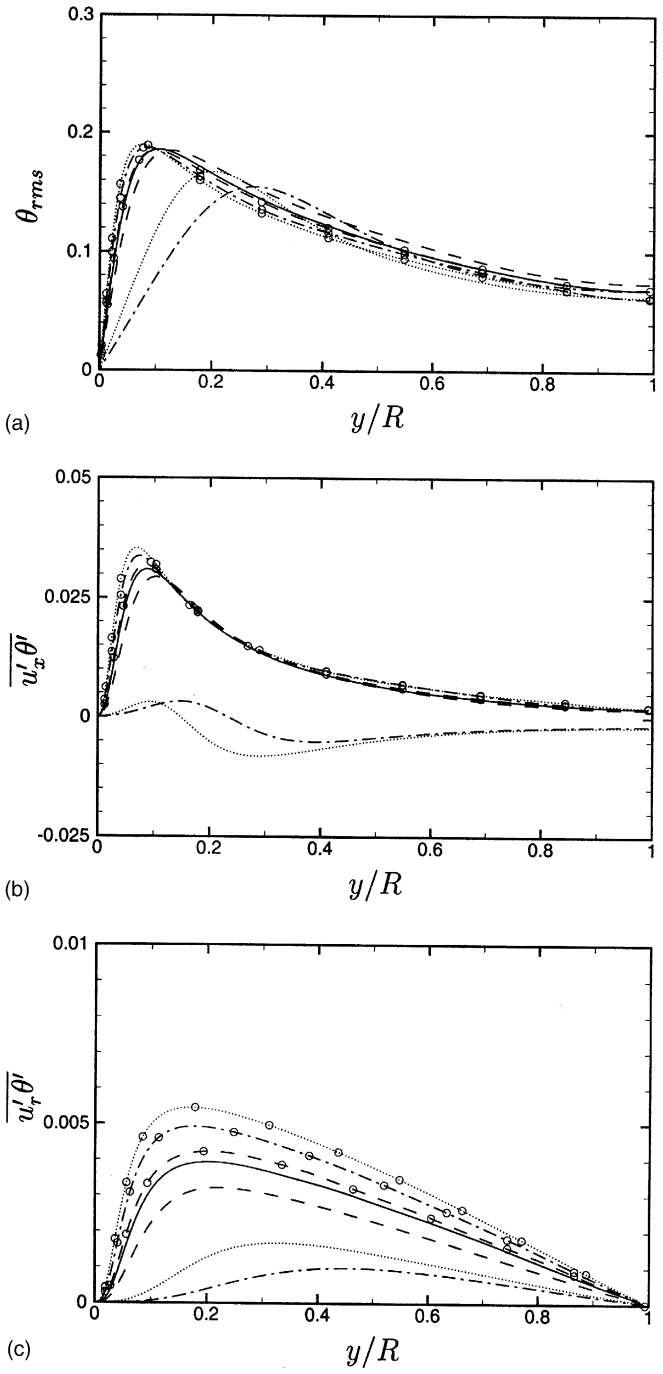

Fig. 7. Temperature fluctuations and turbulent heat fluxes plotted in global coordinates: (a) θ_{rms}; (b) $\overline{u_x'\theta'}$; (c) $\overline{u_r'\theta'}$. Upward heated flow (lines without O): (——) $Gr_q/Re^2 = 0$; (- - - -) 0.063; (-·-·-·) 0.087; (·····) 0.241. Downward heated flow (lines with O): (- - - -) $Gr_q/Re^2 = 0.063$; (-·-·-·) 0.241; (·····) 0.434.

acts as a loss, but it is comparable to the shear production and acts as a gain away from the wall because $\overline{u_x'\varphi'}$ changes its sign across the tube in upward heated flow (Fig. 7b). The buoyancy production is balanced with the dissipation in the region where the shear production becomes small due to the M-shape of the mean

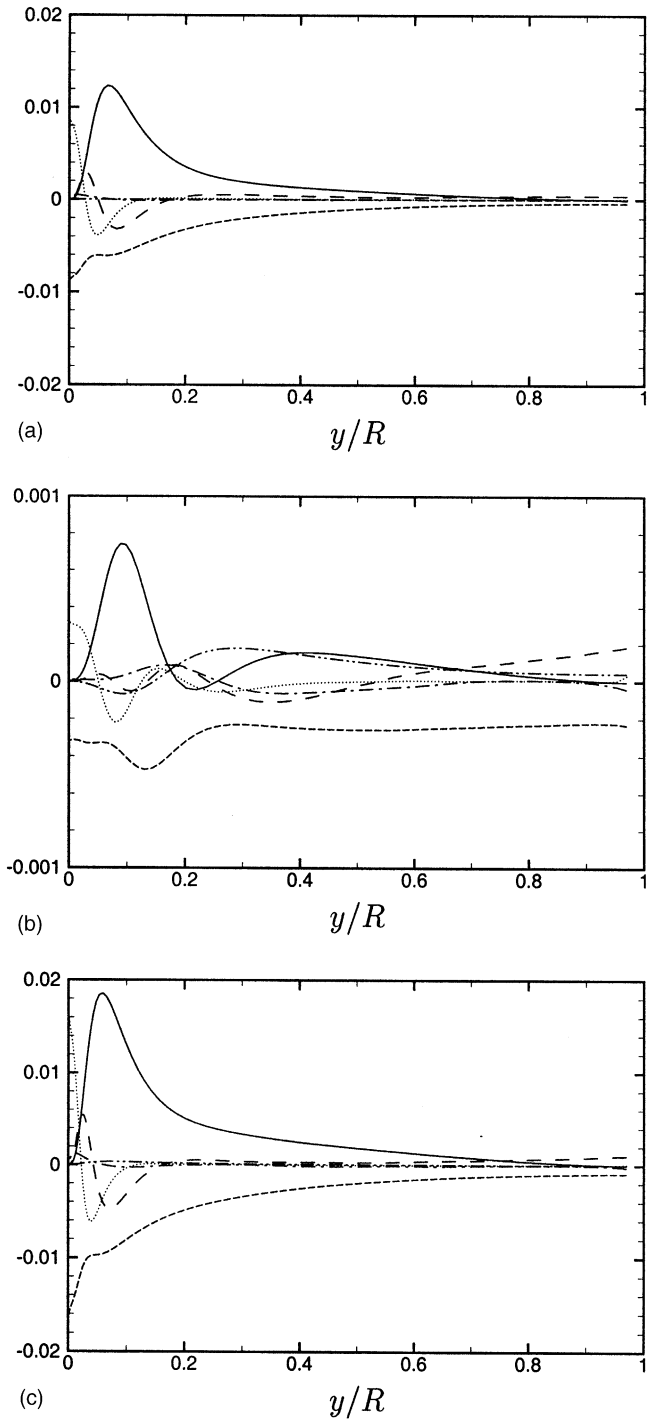

Fig. 8. Turbulent kinetic energy budget: (a) $Gr_q/Re^2 = 0$; (b) 0.241 (upward heated flow); (c) 0.241 (downward heated flow). (——) Shear production; (– –) turbulent diffusion; (-·-·-·) velocity–pressure gradient; (· · · · · ·) viscous diffusion; (- - - -) dissipation; (-·-·-·) buoyancy production. Note that the ordinate scale in (b) is different from those in (a) and (c).

velocity. In downward heated flow, all terms in Eq. (8) increase monotonically with increasing heat flux. The shape of each term is very similar to that for forced convection (Fig. 8c). For example, the maximum dissipation still occurs at the wall. The buoyancy production is very small compared to other terms and acts as a gain

across the tube cross-section because $\overline{u'_x\varphi'}$ is positive in downward heated flow (Fig. 7b).

4.6. Turbulence structure

Fig. 9 shows contours of the instantaneous streamwise vorticity (ω_x) and correlation coefficient of the streamwise velocity and temperature ($u'_x\theta'/u_{x_{\rm rms}}\theta_{\rm rms}$). Without buoyancy (Fig. 9a), strong vortical structures are observed in the near-wall region and the velocity and temperature fluctuations are positively correlated. The statistically averaged value of $u'_x\theta'/u_{x_{\rm rms}}\theta_{\rm rms}$ becomes very close to unity near the wall, which indicates that the thermal streaky structure has the strong similarity to the

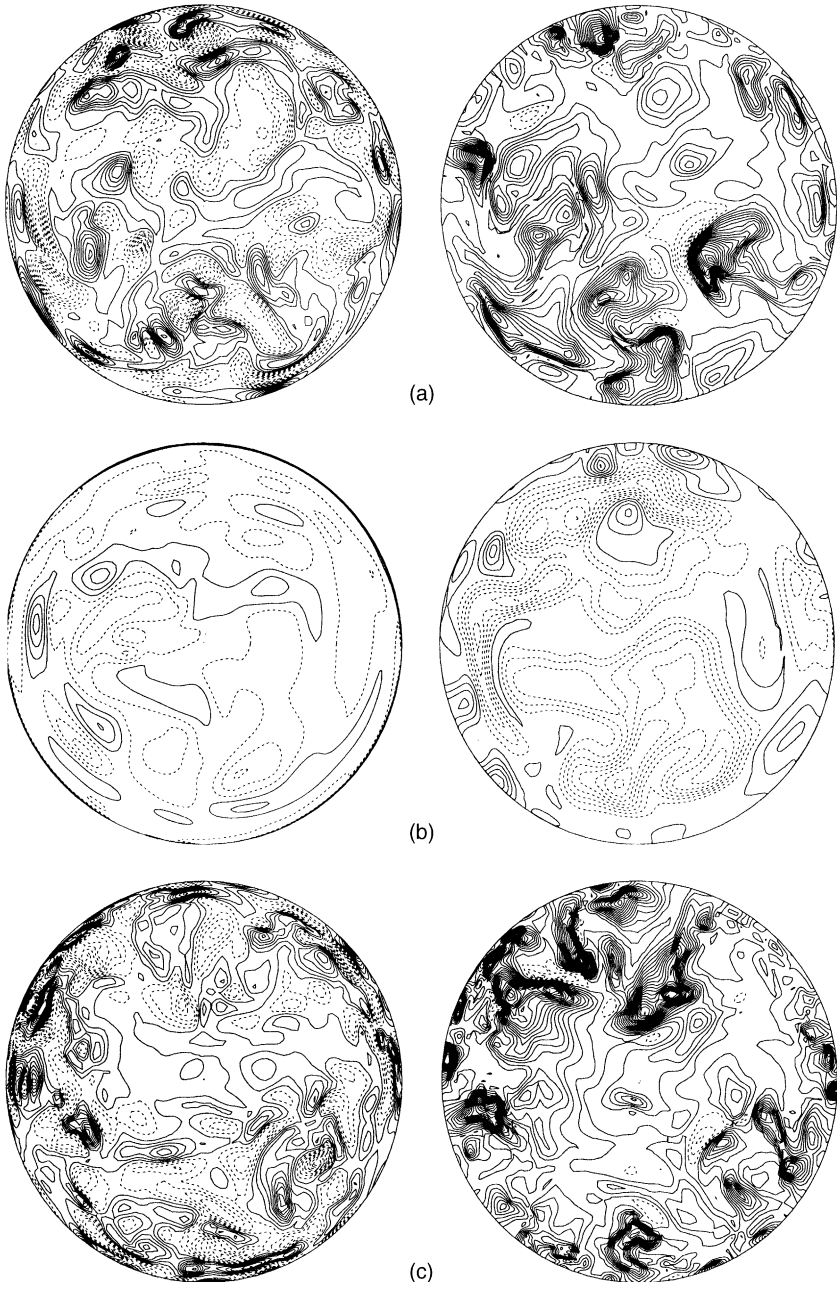

Fig. 9. Contours of the instantaneous streamwise vorticity (ω_x, left) and correlation coefficient ($u'_x\theta'/u_{x_{\rm rms}}\theta_{\rm rms}$, right) at $Gr_q/Re^2 = 0.241$: (a) forced convection, (b) upward heated flow, (c) downward heated flow. Contour levels are from −3 to 3 by increments of 0.24 for ω_x and from −3 to 8 by increments of 0.37 for $u'_x\theta'/u_{x_{\rm rms}}\theta_{\rm rms}$. Dashed contours denote negative values.

momentum one in the near-wall region. Actually, the mean momentum streak spacing obtained from the two-point correlation of the streamwise velocity is nearly the same as the thermal streak spacing. For upward heated flow (Fig. 9b), near-wall vortical structures become weakened in strength and larger in size. The streamwise velocity and temperature fluctuations are negatively correlated except in the near-wall region, which was confirmed with the streamwise turbulent heat flux (Fig. 7b). Also, the value of $\overline{u_x'\theta'}/u_{x_{\rm rms}}\theta_{\rm rms}$ becomes about 0.5 near the wall, indicating that the similarity between the streamwise velocity and temperature is reduced significantly. The momentum streak spacing near the wall increases by 27%, whereas the thermal one increases by 82%. For downward heated flow (Fig. 9c), near-wall vortical structures become stronger and the streamwise velocity and temperature fluctuations have stronger correlations than for forced convection.

As expected from the results in this section, the two-point correlation decays slowly with increasing heat flux for upward heated flow at $Gr_q/Re^2 \leqslant 0.087$, indicating that the integral scale and Taylor micro-scale increase with increasing heat flux. At $Gr_q/Re^2 = 0.241$, due to enhanced turbulence, the two-point correlation decays much faster than that at $Gr_q/Re^2 = 0.087$. On the other hand, the two-point correlation for downward heated flow shows faster decay than for forced convection (not shown in this paper).

4.7. Buoyancy effect on turbulent mixed convection

In laminar mixed convection (Section 3), the velocity near the wall monotonically increases and decreases, respectively, in upward and downward heated flows due to buoyancy. However, in turbulent mixed convection, changes in the velocity are quite different. With increasing heat flux, the velocity near the wall first decreases and then increases in upward flow, while little changes occur in downward flow. Clearly, this difference between laminar and turbulent mixed convection is due to the buoyancy effect on the velocity fluctuations.

Petukhov and Polyakov [16] presented a mathematical expression for upward and downward heated flows and concluded that the influence of buoyancy on turbulent transport is determined by two distinct effects. The first is that buoyancy directly affects the mean velocity, and the second is that it affects the velocity fluctuations. They called the former as an 'external' effect and the latter as a 'structural' effect.

Depending on the amount of heat flux and flow direction, both effects may be commensurable, or one of them may be predominant. From the present result we can give a more detailed account of the external and structural effects. In the case of upward heated flow at low heat fluxes, the mean velocity very near the wall decreases, indicating that the structural effect is dominant there because the external effect causes the mean velocity to increase as in laminar mixed convection. On the other hand, the external effect is dominant in the region away from the wall, so that the mean velocity increases and decreases, respectively, at $r \approx 0.2$ and near the tube center. Above some level of heat flux, where the profiles of the mean velocity, turbulence intensities and Reynolds shear stress are similar to those of turbulent free convection, the external effect is dominant all over the tube cross-section. In the case of downward heated flow, both effects are of the same order.

5. Summary and conclusion

Direct numerical simulations of heated vertical air flows in fully developed turbulent mixed convection have been carried out in the present study. In upward heated flow, the velocity near the wall first decreased and then increased with increasing heat flux. However, in downward heated flow, it changed little from that of the forced convection. The mean-velocity profiles plotted in wall coordinates indicated that the log law used in two-equation turbulence models is valid for downward heated flow but is not for upward heated flow.

Both the skin-friction coefficient C_f and the heat transfer coefficient Nu first decreased and then increased with increasing heat flux in upward heated flow, but at a certain heat flux (e.g., at $Gr_q/Re^2 = 0.241$) $C_f > C_{f_0}$ and $Nu < Nu_0$. In the case of downward heated flow, C_f was nearly unchanged but Nu increased with increasing heat flux. These results clearly showed a dissimilarity between the velocity and temperature due to buoyancy.

The influence of buoyancy on turbulent transport was characterized by the external and structural effects. It was shown that the structural effect is dominant near the wall at low heat fluxes in upward heated flow.

Acknowledgements

The present work was supported by the National Creative Research Initiatives and the National Nuclear Technology Program, of the Ministry of Science and Technology and by the Brain Korea 21 Project of the Ministry of Education and Human Resources Development, Republic of Korea.

References

[1] Y. Parlatan, N.E. Todreas, M.J. Driscoll, Buoyancy and property variation effects in turbulent mixed convection of water in vertical tubes, ASME J. Heat Transfer 118 (1996) 381–387.

[2] J.D. Jackson, M.A. Cotton, B.P. Axcell, Studies of mixed convection in vertical tubes, Int. J. Heat Fluid Flow 10 (1) (1989) 2–15.
[3] B.S. Petukhov, B.K. Strigin, Experimental investigation of heat transfer with viscous-inertial-gravitational flow of a liquid in vertical tubes, High Temp. 6 (5) (1969) 896–899 (in English).
[4] A.D. Carr, M.A. Connor, H.O. Buhr, Velocity, temperature, and turbulence measurements in air for pipe flow with combined free and forced convection, ASME J. Heat Transfer 95 (1973) 445–452.
[5] A.F. Polyakov, S.A. Shindin, Development of turbulent heat transfer over the length of vertical tubes in the presence of mixed air convection, Int. J. Heat Mass Transfer 31 (5) (1988) 987–992.
[6] A.M. Abdelmeguid, D.B. Spalding, Turbulent flow and heat transfer in pipes with buoyancy effects, J. Fluid Mech. 94 (2) (1979) 383–400.
[7] J.P. Easby, The effect of buoyancy on flow and heat transfer for a gas passing down a vertical pipe at low turbulent Reynolds numbers, Int. J. Heat Mass Transfer 21 (1978) 791–801.
[8] N. Kasagi, M. Nishimura, Direct numerical simulation of combined forced and natural turbulent convection in a vertical plane channel, Int. J. Heat Fluid Flow 18 (1997) 88–99.
[9] K. Akselvoll, P. Moin, Large eddy simulation of turbulent confined coannular jets and turbulent flow over a backward facing step, Mech. Eng. Dept. Report TF-63, Stanford University, Stanford, CA, 1995.
[10] P.R. Spalart, Hybrid RKW3 + Crank–Nicolson scheme, Internal Report, NASA—Ames Research Center, Moffett Field, CA, 1987.
[11] M.A. Cotton, I.D. Nott, Computation of developing turbulent mixed convection heat transfer to air in a vertical tube: comparison of a low-Reynolds-number $k-\epsilon$ turbulence model with recent experiments, Anglo-Soviet Seminar on Turbulent Convection, Institute for High Temperatures of the U.S.S.R. Academy of Sciences, Moscow, 1989.
[12] T.J. Hanratty, E.M. Rosen, R.L. Kabel, Effect of heat transfer on flow field at low Reynolds numbers in vertical tubes, Ind. Eng. Chem. 50 (5) (1958) 815–820.
[13] J.G.M. Eggels, F. Unger, M.H. Weiss, J. Westerweel, R.J. Adrian, R. Friedrich, F.T.M. Nieuwstadt, Fully developed turbulent pipe flow: a comparison between direct numerical simulation and experiment, J. Fluid Mech. 268 (1994) 175–209.
[14] B.P. Axcell, W.B. Hall, Mixed convection to air in a vertical pipe, Proceedings of the Sixth International Heat Transfer Conference, Toronto, Canada, 1978, pp. 37–42.
[15] W.B. Hall, J.D. Jackson, Laminarization of a turbulent pipe flow by buoyancy forces, ASME Paper 69-HT-55, 1969.
[16] B.S. Petukhov, A.F. Polyakov, Heat Transfer in Turbulent Mixed Convection, Hemisphere Publishing Corporation, New York, 1988 (pp. 41–55).
[17] A. Steiner, On the reverse transition of a turbulent flow under the action of buoyancy forces, J. Fluid Mech. 47 (1971) 503–512.